

## Venus Express/VIRTIS observations of middle and lower cloud variability and implications for dynamics

K. McGouldrick,<sup>1</sup> K. H. Baines,<sup>2</sup> T. W. Momary,<sup>2</sup> and D. H. Grinspoon<sup>1</sup>

Received 1 February 2008; revised 27 June 2008; accepted 20 August 2008; published 18 November 2008.

[1] We present an analysis of Venus Express Visible and Infrared Thermal Imaging Spectrometer (VIRTIS) data, carried out to characterize the morphological, geographical, and evolutionary trends of the middle and lower cloud features that are observed in the atmosphere of Venus as variations in brightness temperatures in specific near-infrared wavelengths. In this preliminary study, we analyze only data collected over the span of 11 orbits. The mean radiance as a function of latitude is consistent with previous ground-based observations, indicating that the overall global distribution of mean cloud cover is stable, at least on a 10- to 20-year time scale. In contrast with the consistent level of radiance at high latitudes, a significant amount of variability to the radiance exists at lower latitudes, consistent with significant convective activity in the lower and middle cloud decks. The morphology of the holes tends from highly variable orientations of features with aspect ratios of nearly one at low latitudes, to very large aspect ratios and zonally oriented features at higher latitudes. The peak radiance of the holes appears not to demonstrate a latitudinal tendency. There is evidence of more variability to the morphology and radiance of features at lower latitudes. To investigate the evolution of the holes, we examine a sequence of images taken over a 5 h span of a single orbit. If this limited amount of data is representative, then the typical e-folding time scale for the evolution of a hole is about 1 day.

**Citation:** McGouldrick, K., K. H. Baines, T. W. Momary, and D. H. Grinspoon (2008), Venus Express/VIRTIS observations of middle and lower cloud variability and implications for dynamics, *J. Geophys. Res.*, *113*, E00B14, doi:10.1029/2008JE003113.

### 1. Introduction

[2] Holes in the middle and lower cloud decks of Venus were first discovered as spatial inhomogeneities in the near-infrared brightness temperatures [Allen and Crawford, 1984]. Thermal emission from the lower atmosphere and surface of Venus escapes through narrow spectral windows among the near-infrared absorption bands of carbon dioxide and water vapor. This emission is scattered by the sulfuric acid cloud decks. From tracking of the features as they traversed the planet and detailed radiative transfer analysis of the spectra of those features, it was recognized that they represented variations in the lower and middle cloud opacity [Crisp *et al.*, 1989].

[3] The clouds are a defining characteristic of the atmosphere of Venus. They completely enshroud the planet between the altitudes of about 50 and 70 km. Consequently, except for the variations noted in the previous paragraph, the clouds render the lower atmosphere difficult to observe in infrared, visible, and ultraviolet wavelengths. The clouds of Venus have been implicated as playing a significant role

in the maintenance of the Venus greenhouse effect [Pollack *et al.*, 1980]. Thus, breaks in the clouds, which allow a greater flux of radiation to escape (and absorb a smaller amount of solar radiation), can have a significant effect on the thermal balance of Venus. This can have significant ramifications, especially in terms of the long-term climate evolution of Venus [Crisp, 1989; Hashimoto and Abe, 2000; Bullock and Grinspoon, 2001].

[4] The atmosphere of Venus exhibits a global superrotation at most altitudes. In order to sustain the global superrotation, there must be vertical transport of horizontal momentum to the upper atmosphere, specifically between about 40 and 80 km. Vertical transport of momentum by eddies and by waves has been suggested [Schubert *et al.*, 1980]. However, both the eddies and the waves are going to interact in some way with the clouds that occupy the altitudes between 50 and 70 km. Most likely, vertically traveling waves and eddies will be dissipated by the regions of instability in the vicinity of the clouds. The radiative dynamical feedback that supports the cloud [Pollack *et al.*, 1980; McGouldrick and Toon, 2007], maintains a region of dynamic instability in the middle and lower cloud region, which can limit the efficiency of vertical momentum transport by wave propagation. The shear profile and the static stability profile, both of which affect the vertical transport of energy that is brought about by convection, will have the largest effect on what happens to these vertically propagating waves and eddies. Furthermore, the morphological appear-

<sup>1</sup>Department of Space Sciences, Denver Museum of Nature and Science, Denver, Colorado, USA.

<sup>2</sup>Jet Propulsion Laboratory, California Institute of Technology, Pasadena, California, USA.

ance of cloud features (aspect ratio and “tilt” relative to the zonal direction) can offer information on the nature of these atmospheric characteristics (shear profile, static stability profile, and the amount of convective overturning). Thus, the morphology of the clouds can provide insight to the dynamical environment; hence, the efficiency of vertical momentum transport by these processes.

[5] For these reasons, an understanding of what sustains the clouds, and what sorts of changes are responsible for the formation of holes in those clouds, is necessary in order to understand the Venus atmosphere as a whole. In this paper, we compare the results and predictions of several recent theoretical studies of the clouds of Venus, to recent observations made by the Visible and Infrared Thermal Imaging Spectrometer (VIRTIS) on Venus Express. We analyze the possible existence of latitudinal tendencies of cloud morphology and overall cloud opacity, as well as the typical cloud feature lifetimes.

### 1.1. Previous Observations of the Clouds and Holes

[6] *Crisp et al.* [1989] showed that the near-infrared features discovered by *Allen and Crawford* [1984] were caused by variations in the opacity of the middle and lower cloud decks. The observations by *Crisp et al.* [1989] also provided an early general characterization of the morphology and distribution of the cloud features at wavelengths of 1.74  $\mu\text{m}$  and 2.3  $\mu\text{m}$  in the near infrared. *Crisp et al.* [1989] observed an apparent latitudinal dependence of the overall cloud opacity, in which the opacity was greatest at high latitudes, and a relatively featureless bright band associated with diminished cloud opacity that often existed at mid latitudes (around 40° to 60°). *Crisp et al.* [1989] also noted occasional significant asymmetry between the brightness (hence, opacity) of the northern and southern hemispheres.

[7] The flyby of the Galileo spacecraft in February of 1990 provided an excellent opportunity for the study of these near-infrared cloud features. *Belton et al.* [1991] observed the clouds of Venus with the Galileo solid-state imaging (SSI) camera. It is important to note, however, that the features observed by SSI likely are due to cloud variability at a higher altitude (i.e., about 60 to 65 km) than the cloud variability observed in the near-infrared spectral windows on the nightside (i.e., around 50 to 55 km). This is partly because the dayside observations detected solar infrared radiation that has been reflected from near the tops of the clouds, whereas the nightside observations detected surface-emitted infrared radiation transmitted through the clouds from below. Gaseous absorption by the atmosphere extinguishes the emitted or reflected radiation at much higher altitudes outside of the narrow spectral windows. Thus, the broadband observation exhibits contributions from a greater range of altitudes (mostly higher) than does the narrow-band observation. Nevertheless, *Belton et al.* [1991] noted that cloud features tended to appear “patchy” at low latitudes and “streaky” at high latitudes. Viewing the cloudy atmosphere at spatial resolutions as fine as 17 km per pixel, *Belton et al.* [1991] detected changes in cloud morphology on time scales only in excess of an hour or two; generally on the order of 1 day. They also noted the presence of “bright-rimmed cellular features,” suggestive of cellular convective elements that had lifetimes in excess of a day, and sizes on the order of a few hundred kilometers.

*Blamont et al.* [1986] also noted a tendency of cloud features at higher latitudes to tilt relative to the zonal direction in a way that suggested a spiral pattern. Such a spiral (i.e., the polar vortex) is known to exist over both the north and south poles of Venus [*Taylor et al.*, 1979; *Piccioni et al.*, 2007]. The latitudinal extent of the *Piccioni et al.* [2007] observations is only poleward of about 50° latitude. Analysis of the tilting of cloud features in images centered over middle and lower latitudes can place constraints on the equatorward influence of these polar vortices.

[8] *Carlson et al.* [1991], observing the nightside of Venus with the Galileo Near-Infrared Imaging Spectrometer (NIMS), noted that contrast between the brightest and darkest regions of the nightside of Venus at 1.74  $\mu\text{m}$  was about 5:1. *Carlson et al.* [1991] also noted the existence of linear features whose tilt relative to the parallels of latitude implied meridional transport, presumably by Hadley circulation. These features seem to be similar in appearance to those described by *Blamont et al.* [1986] and *Belton et al.* [1991]; but *Carlson et al.* [1991] noted that establishment of a direct correlation of features between the two instruments (NIMS and SSI) was uncertain.

[9] While the Galileo Near-Infrared Mapping Spectrometer (NIMS) was able to obtain only, essentially, a snapshot of the planet during the flyby, ground-based observations by *Crisp et al.* [1991a], spanning the weeks leading up to and following the flyby, were able to provide some context for the NIMS observations. *Crisp et al.* [1991a] detected a latitudinal distribution of cloud opacity similar to that observed by *Crisp et al.* [1989]. That is, they noted that high-latitude regions tended to be “dark and featureless,” whereas midlatitude regions tended to be “occupied by bright quasi-zonal bands.” In addition, low latitudes were noted to exhibit the most variability, both in terms of feature opacity and size. *Crisp et al.* [1991a] also noted the existence of a very large (hemisphere-scale) dark region that had persisted throughout the duration of the observing sessions (about 7 weeks). *Chanover et al.* [1998] also noted the existence of such a hemispherical asymmetry. Finally, *Crisp et al.* [1991a] noted that the features that were visible to Galileo during the flyby were of a relatively small scale that tended not to persist for more than about a week (i.e., about one atmospheric rotational period).

[10] *Markiewicz et al.* [2007b] described observations of Venus cloud structure observed with the Venus Monitoring Camera (VMC) [*Markiewicz et al.*, 2007a] on board Venus Express. While the infrared channels of VMC can be used to probe the middle and lower clouds of Venus, the observations reported by *Markiewicz et al.* [2007b] are mostly in the ultraviolet channel. Thus, their observations are of cloud features located largely above 65 km altitude. They observe the polar vortex as a dark spiral structure in the ultraviolet images. They observe a mottled cloud structure at low latitudes, which they attribute to vigorous convection in the upper cloud deck, with the sizes of typical convective cells being about 30 km. They also report waves with wavelengths on the order of 10 to 30 km in the upper cloud region.

### 1.2. Previous Simulations of the Clouds and Holes

[11] Simulations suggest that the global dynamics of Venus have a significant effect on the formation and distribution of the Venus clouds and their holes. *Imamura*

and Hashimoto [1998] showed that the Hadley circulation could result in enhancements of cloud opacity in the vicinity of both the ascending branch and the descending branch of the near-global Hadley cell. *McGouldrick and Toon* [2008b] showed that differences in the structure of the vertical shear of the zonal winds could have an effect on the evolution of large ( $\sim 2000$  km) holes in the clouds of Venus. *McGouldrick and Toon* [2008a] showed that convective cells with typical size and separation of about 30 km tended to generate holes with lifetimes on the order of an hour or two, and with optical depths that were consistent with observations. *McGouldrick and Toon* [2008a] also showed that gravity waves, with characteristics similar to those of waves putatively launched by convection that have been both observed [*Hinson and Jenkins*, 1995] and simulated [*Baker et al.*, 2000], can generate wave-like features in the clouds with  $\sim 10$  to  $\sim 30$  km wavelengths, visible in the emitted  $1.74 \mu\text{m}$  radiation.

[12] *Imamura and Hashimoto* [1998] suggested that the Hadley circulation determines the latitudinal variation in the middle and lower cloud deck opacity. Upwelling in the ascending branch near the equator leads to enhanced opacity because of the influx of sulfuric acid vapor into the cloud region. Meridional transport toward the descending branch of the Hadley circulation, which they reasoned to occur poleward of  $55^\circ$  latitude, also leads to enhanced cloud opacity because of an accumulation of upper cloud mass that has been transported poleward by the upper level Hadley circulation (because the time scale for the sedimentation of the upper cloud particles was considerably longer than the time scale for poleward transport of those particles by the Hadley circulation). Furthermore, the bright region between about  $40^\circ$  and  $60^\circ$  latitude could be explained as an absence of these cloud-thickening mechanisms. They also found that if the Hadley circulation were slower, then the contrast between the brightness at midlatitudes and that at high latitudes would be less severe, as a result of a thinning of the upper cloud at high latitudes. If the Hadley circulation were less efficient, then the time for the upper level flow to travel from equator to pole no longer would be large compared with sedimentation times of the upper cloud particles. Hence, less photochemically produced mass is transported to high latitudes. They also found that the bright band was located more equatorward in the case of a less efficient Hadley circulation. Hence, it may be possible to determine the magnitude of the Hadley circulation by determining the latitudinal location of the high-latitude peak in total cloud opacity [*Imamura and Hashimoto*, 1998].

[13] The middle and lower cloud decks of Venus are sustained by a radiative dynamical feedback, whereby heating of the cloud base by the very warm deep atmosphere drives an unstable lapse rate within the region occupied by the middle and lower cloud decks [*McGouldrick and Toon*, 2007]. Furthermore, the time scales for growth and for dynamical transport (by winds, and by convection, when present) are much shorter than the radiative time scale. Hence, in the simulations by *McGouldrick and Toon* [2007], the structure of the clouds was dominated by brief, intense periods of vertical transport (i.e., convection), separated by longer periods of quiescence during which the thermal instability developed.

[14] *McGouldrick and Toon* [2008b] suggested that the nature of the vertical wind profile affects the longevity and possibly the morphology of large holes ( $\sim 2000$  km) in the clouds. Specifically, the vertical shear of the zonal wind, coupled with the radiative dynamical feedback, can effectively dissipate large holes in the clouds. Furthermore, the nature of the vertical shear profile affected the time required to smooth out a simulated hole in the clouds. In simulations exhibiting negligible vertical shear throughout the middle cloud deck (as have been observed at low latitudes and midlatitudes by Pioneer Venus [*Counselman et al.*, 1980] and measured via multispectral wind tracking with VIRTIS on board Venus Express [*Sánchez-Lavega et al.*, 2008]), the lifetimes of holes were longer than in simulations in which the shear was at a constant magnitude throughout the entire cloud domain (i.e., shear similar to what has been observed at higher latitudes, especially by the Pioneer Venus north probe). Although the radiative dynamical feedback was able to limit the zonal “stretching” of holes in the simulations by *McGouldrick and Toon* [2008b] that exhibited minimal shear within the middle and lower cloud decks, the holes were stretched out across large zonal distances in simulations that exhibited greater amounts of shear. Such differences in the aspect ratios of features in the Venus clouds observed by VIRTIS could indicate the vertical structure of the zonal winds in the region of the middle and lower cloud decks of Venus. That is, holes that become highly zonally elongated may be in regions of high vertical shear of the zonal wind; and holes that maintain a more blocky appearance may be in regions of low vertical shear of the zonal wind.

[15] An alternative cause for this zonal stretching of cloud features could be horizontal shear of the zonal wind. However, observations by both the Venus Monitoring Camera and VIRTIS on Venus Express indicate that there is negligible meridional shear of the zonal wind equatorward of about  $50^\circ$  latitude [*Markiewicz et al.*, 2007b; *Sánchez-Lavega et al.*, 2008]. Thus, at latitudes equatorward of  $50^\circ$ , the only contribution to stretching by the meridional shear of the zonal wind arises from the change in planetary circumference with latitude ( $\phi$ ):

$$\frac{\partial \omega}{\partial \phi} = \frac{86400 u \tan \phi}{R_V \cos \phi}, \quad (1)$$

where  $R_V = 6100 \times 10^3$  m is the radius of the planet at the altitude of the clouds,  $\omega$  is the angular velocity of the atmosphere in units of  $^\circ$  longitude per day, and the factor 86400 is needed to convert the units of the RHS to  $\text{day}^{-1}$ . For  $\phi \leq 50^\circ$ , and  $u = 60 \text{ m s}^{-1}$  from *Sánchez-Lavega et al.* [2008], this rate does not exceed  $1.6^\circ$  longitude per day per degree of latitude. Thus, among features at midlatitudes to low latitudes, only those holes that persist for several days, can be stretched significantly by the meridional shear. Furthermore, the stretching of the cloud features cannot be the result of zonal shear of the zonal wind. Such a situation would result in horizontal convergence or divergence, which would force vertical motion of atmospheric parcels. Such vertical motion can create significant changes in cloud opacity [*McGouldrick and Toon*, 2007, 2008a], but will not cause a zonal elongation of the features.

[16] *McGouldrick and Toon* [2008a] analyzed the effect of gravity waves and convection cells on the appearance of

**Table 1.** Data Analyzed in Morphological Analyses

File Name	Orbit	Start Date	Start Time <sup>a</sup>	Exposure Time <sup>b</sup> (s)	Distance (km)
VI0363_00	363	18 Apr 2007	2017:56	0.36	67021.2
VI0364_00	364	19 Apr 2007	2017:10	3.3	66775.9
VI0365_00	365	20 Apr 2007	2016:25	0.36	66468.1
VI0366_00	366	21 Apr 2007	2015:42	3.3	66226.3
VI0367_00	367	22 Apr 2007	2014:57	0.36	67209.0
VI0368_00	368	23 Apr 2007	2014:12	3.3	67226.6
VI0369_00	369	24 Apr 2007	2013:25	0.36	67218.5
VI0370_00	370	25 Apr 2007	2012:41	3.3	67223.6
VI0371_00	371	26 Apr 2007	2011:55	0.36	67203.3
VI0372_00	372	27 Apr 2007	2011:10	3.3	67220.6

<sup>a</sup>Times and dates are UTC.

<sup>b</sup>Exposure time is per slice.

the clouds of Venus. They found, from a simple kinematical model used to drive the microphysical model utilized by *McGouldrick and Toon* [2007], that convective cells with sizes on the order of 30 km and vertical velocities of  $\pm 2 \text{ m s}^{-1}$  produce optical depth variations comparable in magnitude to those that have been observed in the clouds of Venus [*Grinspoon et al.*, 1993], and which experience lifetimes on the order of hours. These simulated convective cells are consistent with those that have been observed with the Vega balloons [*Linkin et al.*, 1986], and that have been generated in convective simulations by *Baker et al.* [2000]. *McGouldrick and Toon* [2008a] also found that gravity waves, such as those found in the simulations of *Baker et al.* [2000], and in the occultation observations by *Hinson and Jenkins* [1995], would lead to the appearance of wave-like structures in the lower clouds of Venus, with wavelengths comparable to the size of the convective cells.

### 1.3. VIRTIS

[17] The VIRTIS-M IR channel is a medium (spatial) resolution (0.25 mrad) infrared mapping spectrometer that covers the range of wavelengths from  $1 \mu\text{m}$  to  $5 \mu\text{m}$ , with a spectral resolution of roughly  $\lambda/\Delta\lambda \sim 250$ . This is sufficient spectral resolution to resolve the spectral windows [*Drossart et al.*, 2007]; and the spatial resolution allows for the detection of features as small as about 30 km when the spacecraft is at apoapse ( $d \sim 66,000 \text{ km}$ ). When the spacecraft is within about 10,000 km of the planet during the course of its highly eccentric orbit, it is moving too quickly for VIRTIS to operate very effectively in its mapping modes [*Drossart et al.*, 2007]. Thus, all of the data we analyze in this paper are obtained at spacecraft distances greater than  $\sim 10,000 \text{ km}$ .

[18] With clever pointing over the course of multiple orbits, a significant latitudinal and longitudinal coverage of the clouds of the southern hemisphere may be built up, which allows for the determination of possible latitudinal tendencies in the location of and optical thickness of the clouds. In the course of a single orbit, it is possible to observe several hours worth of cloud evolution (up to about 6 h) of a small region of the Venus atmosphere (defined by the field of view common to all of the images in the series: the maximum possible region being the total field of view of the image taken when the spacecraft is closest to the planet). Analysis of longer-term evolution is possible, but requires a repointing of the spacecraft on successive orbits, since the

previously observed region of the atmosphere will have rotated out of the relatively narrow field of view by the time the spacecraft next arrives in position for observation by the mapping modes of VIRTIS. Even with successive repointings that follow the rotation of the atmosphere, significant changes in cloud morphology during the time that VIRTIS-M is unable to observe the planet frequently make difficult the recovery of features common to observations on successive orbits.

## 2. Observational Goals and Methods

[19] Specific latitudinal variations in overall cloud opacity have been predicted to be a consequence of the Hadley circulation [*Imamura and Hashimoto*, 1998], and have been recorded by ground-based observations [*Crisp et al.*, 1991a]. Does a large-scale latitudinal dependence of cloud cover exist in the VIRTIS data, as suggested by previous ground-based observations? Are there significant spatial or temporal variations in the latitudinal distribution of cloud cover? Tendencies in cloud shape (aspect ratio) and orientation (angle of “long axis,” relative to the zonal direction) can indicate differences in the shear structure or in the level of convection that is occurring. Does a latitudinal tendency to cloud shape or orientation exist in the VIRTIS data? Since the clouds represent a significant contributor to the greenhouse effect on Venus, their variability can alter the thermal balance of the planet. How variable are the clouds, and how does cloud variability affect the thermal balance? We analyze a subset of the VIRTIS-M IR observations to attempt to answer these questions concerning the interactions between the atmospheric dynamics and the cloud structure of Venus.

[20] In all cases, we perform our analyses using the  $1.74 \mu\text{m}$  image of the VIRTIS-M IR data. We choose this wavelength band over those in the other spectral windows because the  $1.74 \mu\text{m}$  band possesses the best combination of high peak radiance and sufficient contrast between cloudy and clear observations; thus, the signal-to-noise ratio of both the brighter holes and the darker clouds is greater than it is for any other spectral image. Furthermore, while the images in the  $2.3 \mu\text{m}$  window region demonstrate a greater overall brightness contrast (around 20:1 in the Galileo NIMS data, compared with a roughly 5:1 ratio at  $1.74 \mu\text{m}$  [*Carlson et al.*, 1991]), the radiance in the cloudiest regions, is barely distinguishable (and possibly indistinguishable) from the background noise. In order to analyze the latitudinal distribution of cloud cover and cloud morphology on Venus, we use images/cubes taken near the apoapse ( $\sim 66,000 \text{ km}$ ) of several successive orbits (orbits 363 through 372), as summarized in Table 1. We use images obtained near apoapse in order to maximize our spatial coverage of the planet, with only a small loss in spatial resolution. The data are calibrated using the VIRTIS PDS/IDL software library, as described by *Drossart et al.* [2007].

[21] Figure 1a demonstrates the overall coverage of the middle atmosphere by these selected observations. In generating this plot, we assume that the atmosphere rotates at a solid body rate of once per 5.5 days (a speed of about  $80 \text{ m s}^{-1}$  at the equator, or about  $60 \text{ m s}^{-1}$  at  $40^\circ$  latitude), and shift the geographic longitudes of each observation to the east, according to the time separation of each image from

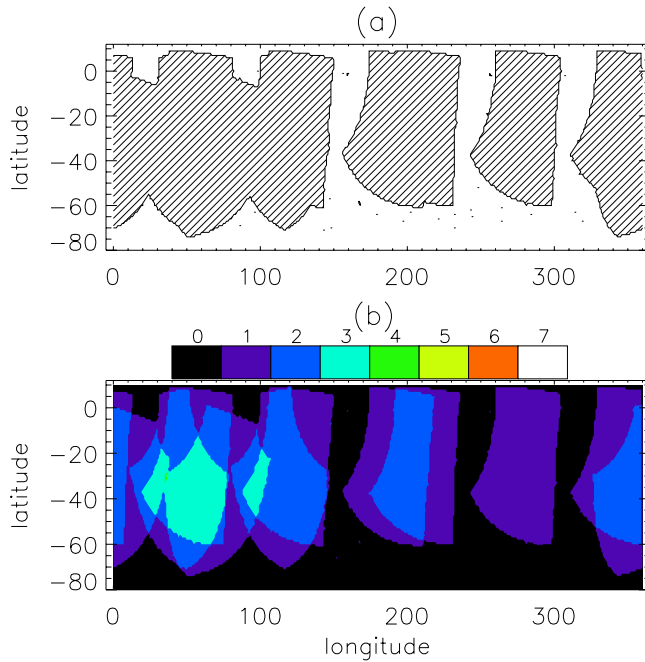


**Figure 1.** Distribution and frequency of coverage of the atmosphere by the images analyzed in this paper. (a) The regions of the atmosphere that have been imaged at least once over the course of the considered images (crosshatched regions). (b) The frequency of coverage of the atmosphere. The numbered contours indicate the number of images among those considered here that view the same region of the atmosphere. Both plots assume the atmosphere rotates as a solid body with a period of 5.5 days.

the first image (orbit 363). We choose a planet-circling period of 5.5 days for the clouds because that period is consistent with previous observations of lower and middle cloud tracking [Allen and Crawford, 1984; Crisp *et al.*, 1991b]. According to the recent analysis of wind speeds from VIRTIS data by Sánchez-Lavega *et al.* [2008], a zonal wind speed of about  $80 \text{ m s}^{-1}$  corresponds to an altitude between 58 and 70 km, for latitudes equatorward of  $50^\circ$ . A 5.5 day period at  $40^\circ$  latitude is consistent with the  $60 \text{ m s}^{-1}$  winds reported by Sánchez-Lavega *et al.* [2008] at altitudes between 46 and 61 km. Though it is an oversimplification to assume solid body rotation, doing so allows us to obtain at least a first-order estimate of the atmospheric coverage of the observations. It also helps to facilitate the identification of features from image to image, despite their sometimes significant evolution (see section 2). Figure 1a shows that the images that we consider for this particular analysis provide us with coverage of a significant fraction of the southern hemisphere atmosphere (about 72% coverage of the area between the latitudes of  $+10^\circ$  and  $-90^\circ$ , with most of the missing regions lying poleward of  $-70^\circ$ ). This extensive coverage of the atmosphere allows us to have confidence in the conclusions that we draw regarding the latitudinal distributions of the features. If these images did not cover so much of the planet longitudinally, our analyses might have been blind to hemispherical variations such as those that have been reported by Crisp *et al.* [1989, 1991b].

[22] Figure 1b shows the frequency of observations by location in the atmosphere. We see that among these images there is significant overlap, such that about 35% of the atmosphere between  $+10^\circ$  latitude and  $-90^\circ$  latitude has been imaged at least twice; and some regions (such as the one centered near  $50^\circ$  longitude and  $-40^\circ$  latitude) have been observed three times or more. Such repeated coverage of the same part of the atmosphere gives hope to the possibility of ultimately extending the analysis of the variation in feature morphology and evolution from time scales no greater than  $\sim 6 \text{ h}$  (the extent of observation possible during a single orbit) to time scales on the order of days.

## 2.1. Latitudinal Distribution of Cloud Cover and Hole Morphology

[23] Crisp *et al.* [1989, 1991b] noted the appearance of a significant latitudinal distribution of cloud cover in which midlatitudes tended to be brighter, and higher latitudes tended to be darker. Imamura and Hashimoto [1998] provided a theoretical explanation of such a latitudinal distribution of cloud opacity, which, they determined, is caused by the action of the Hadley circulation. Here again, the tremendous volume of the VIRTIS data can play a significant role in confirming or refuting the existence and consistency of such a distribution of cloud opacity. Additionally, the VIRTIS data can be used to more finely tune such simulations of the Hadley circulation on Venus. To analyze the latitudinal distribution of cloud cover, we remap the VIRTIS data to a cylindrical projection and correct for the emission angle by applying the correction used by Carlson *et al.* [1993]. We then find the mean and standard deviation of the radiance as a function of latitude for each image. We also calculate a longer-term average latitudinal distribution of radiance, in which we average over all 10 images considered here.

[24] Belton *et al.* [1991] suggested that there was a trend in the shapes of the features as a function of latitude. Specifically, the features at lower latitudes appeared “blocky,” whereas those at higher latitudes appeared streaky. The great volume of VIRTIS data from Venus Express can indicate whether these trends noted by Belton *et al.* [1991] are real and/or persistent. We investigate these possible morphological tendencies of the clouds by identifying features in each image, and determining a longitudinal versus transverse aspect ratio for each feature. The features are identified by using the latitudinal profile of the mean radiance of each image, as described in section 2.1. We subdivide the image into latitude bands that are no greater than  $15^\circ$  in extent. We find the mean and the standard deviation of the radiance over those latitudes in that image, and draw contours of the mean and the mean plus one standard deviation onto the image (Figure 2). A feature is identified if the mean plus standard deviation contour is closed (or nearly so) and convex. At higher latitudes, where the longitudinal variation is smaller and the latitudinal variation is greater, we use narrower bands to determine the defining contours. We determine the longitudinal versus transverse aspect ratio by measuring the distances along the long and short axes of each feature. The feature is assigned latitude and longitude coordinates that identify its left (L), right (R), top (T), and bottom (B) extent. The aspect ratio is then the ratio of the LR arc to the TB arc. Thus, a large aspect ratio indicates a highly elongated feature,

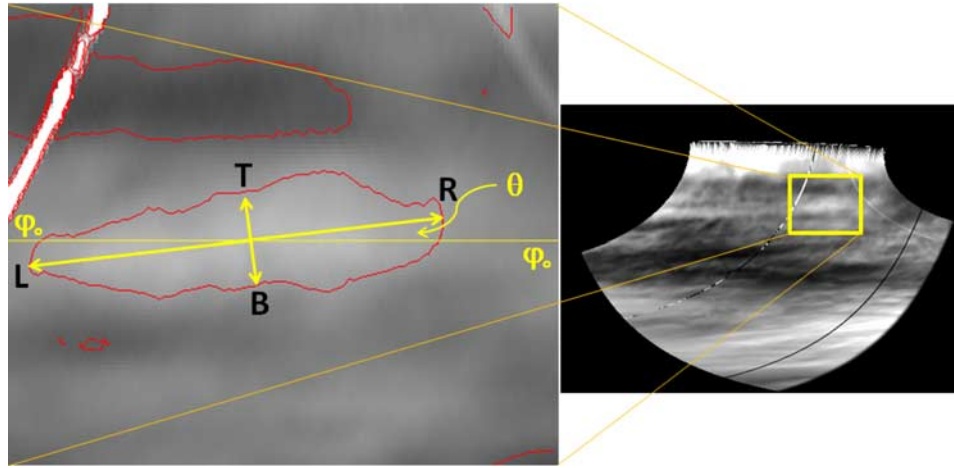


**Figure 2.** (right)  $1.74 \mu\text{m}$  VIRTIS image VI0383\_00. (left) The blowup highlights and zooms in on the boxed region of the VIRTIS image. The parameters measured in the course of the morphological analyses are shown in the zoomed image at left.

whereas an aspect ratio closer to one indicates a more blocky feature.

[25] We also accumulate information on the tilt of the features relative to the parallels of latitude. The tilt angle is taken to be the angle that the LR arc of the feature makes relative to the parallels of latitude. Depending upon the magnitude of the meridional and zonal winds, a tilt measured from the parallels of latitude can indicate meridional flow or shear of cloud material or energy or a significant vertical shear of the zonal wind.

## 2.2. Cloud/Hole Lifetimes

[26] The duration of holes in the clouds of Venus can indicate the nature of the processes that sustain them. *McGouldrick and Toon* [2008b] suggested that differences in the vertical profile of the zonal wind could lead to differences in the longevity of the features. Furthermore, *McGouldrick and Toon* [2008b] noted that a combination of vertical shear of the zonal wind and the vertical motions driven by the radiative dynamical feedback was sufficient to dissipate a large ( $\sim 2000$  km) hole in a time scale of under two weeks. *Crisp et al.* [1991b] reported that a  $\sim 2000$  km hole persisted for at least two weeks. However, since the initial formation of that particular feature was not observed, this is only a lower limit. Furthermore, the spatial resolution of VIRTIS on Venus Express, even at apoapse, is far

superior to what *Crisp et al.* [1991b] were able to achieve from Earth. Thus, the analysis of the evolution of smaller features is now possible. Since the absorption of upwelling infrared radiation plays a role in sustaining the middle and lower clouds [*Pollack et al.*, 1980; *McGouldrick and Toon*, 2007], the longevity of holes affects the magnitude of possible horizontal temperature or pressure variations that would result from such heating. Strong horizontal temperature or pressure gradients will affect the magnitude of vertical motions triggered by the radiative dynamical feedback.

[27] To determine the typical lifetime of the cloud features, we analyze the VIRTIS-M data from orbit 383. This orbit contains a sequence of cubes that spans 5 uninterrupted h, and each cube in the sequence exhibits exposure times long enough that the nightside (rather than the dayside) is exposed ideally (Table 2). Since the Venus Express spacecraft is approaching Venus throughout the series of acquired cubes in each orbit, there is only a small area of the planet's atmosphere, which cannot exceed the field of view of the last cube acquired (i.e., when the spacecraft is at its closest to Venus), that contains features that can be tracked for the entirety of the sequence.

[28] We first identify features that persist throughout the series of observations. That is, we limit our analysis to features that persist for at least 5 h, and do not stray beyond the instrumental field of view. The zonal superrotation

**Table 2.** Data Analyzed in Evolution Analyses

File Name	Orbit	Start Date	Start Time <sup>a</sup>	Exposure Time <sup>b</sup> (s)	Distance (km)	Resolution (km pixel <sup>-1</sup> )
VI0383_00	383	8 May 2007	2028:12	3.3	67106.1	16.8
VI0383_01	383	8 May 2007	2058:12	3.3	66178.0	16.5
VI0383_02	383	8 May 2007	2128:12	3.3	65055.9	16.3
VI0383_03	383	8 May 2007	2158:12	3.3	63735.1	15.9
VI0383_04	383	8 May 2007	2228:12	3.3	62426.3	15.6
VI0383_05	383	8 May 2007	2258:12	3.3	60678.6	15.2
VI0383_06	383	8 May 2007	2328:12	3.3	58710.8	14.7
VI0383_07	383	8 May 2007	2358:12	3.3	56515.1	14.1
VI0383_08	383	9 May 2007	0028:12	3.3	54343.1	13.6
VI0383_09	383	9 May 2007	0058:12	3.3	51631.1	12.9
VI0383_10	383	9 May 2007	0128:12	3.3	48668.4	12.2

<sup>a</sup>Times and dates are UTC.

<sup>b</sup>Exposure time is per slice.

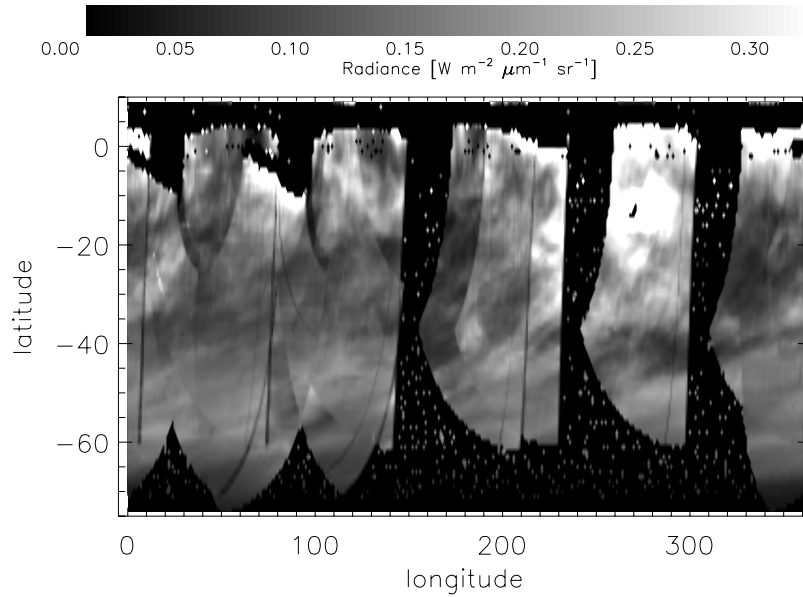


**Figure 3.** All 10 images considered in the morphological analyses, combined into a single image. The atmosphere is assumed to rotate as a solid body, with a planet-circling period of 5.5 days, as in Figure 1.

makes it difficult to be certain of the identity of each feature from image to image, so we crudely correct for the motion of the atmosphere by shifting each image longitudinally at a corresponding rate of about  $2.73^\circ \text{ hr}^{-1}$  (which equates to a 5.5 day period). This adjustment renders many of the features nearly stationary in the sequence of images, thus identification of the same hole in subsequent images was facilitated. The boundary of each feature is determined in the same manner as the feature boundaries in the morphological analysis above (section 2.1). We measure the peak radiance and the contrast between the peak radiance and the background radiance for each feature that we were able to track in this sequence of images.

### 3. Results

#### 3.1. Latitudinal Distribution of Cloud Cover

[29] Figure 3 demonstrates the approximate spatial coverage of cloudy and clear regions in the data considered in this paper. All of the considered  $1.74 \mu\text{m}$  images are plotted onto a cylindrical projection. As in Figure 1, the atmosphere is assumed to rotate as a solid body with a period of 5.5 days, so each image has been advected longitudinally according to the time it was acquired relative to the first image (orbit 363). Overlapping regions are averaged together. There is possibly a hint of longitudinal hemispherical asymmetry, similar to that observed by *Crisp et al.* [1991a], whereby longitudes east of  $180^\circ$  in these data are brighter than those west of  $180^\circ$ ; but this conclusion might be biased by the existence of a single very large and very bright feature that spans the region from  $220^\circ$  to  $300^\circ$  longitude and  $-20^\circ$  to  $-5^\circ$  latitude. Although the data cover nearly two full atmospheric rotations, the coverage and consistency seems to be insufficient to determine whether a longitudinal hemispherical asymmetry exists in these data.

[30] Figure 4 shows the latitudinal profile of the mean radiance for each of the images considered in this paper as

well as the overall mean and standard deviation of all of the data considered here. The overall mean indicates that the 10 images that we have analyzed for this paper demonstrate the same tendencies that have been noted by previous

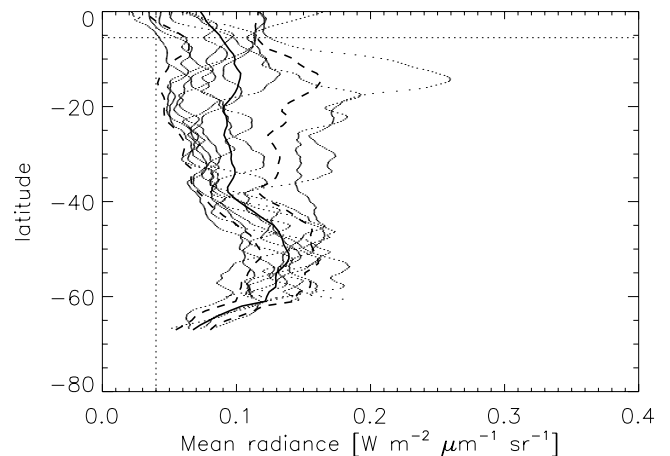


**Figure 4.** Latitudinal profile of the mean radiance for each of the  $1.74 \mu\text{m}$  images considered in this paper. The profiles of the various images are plotted as points. The mean of all of the data considered is shown as a solid line, and range of  $\pm 1$  standard deviation of all of the data considered is shown with a pair of dashed lines. Also shown here, for comparison, is an estimate of the emitted radiance that results from an application of the cloud properties as derived from the Pioneer Venus Lower Cloud Particle Size Spectrometer (LCPS) by *Knollenberg and Hunten* [1980]. The vertical dotted line is the calculated radiance; the horizontal dotted line is the latitude of the probe's descent (the probe actually descended in the northern hemisphere, but we assume roughly hemispherical symmetry only for the purpose of making this comparison).

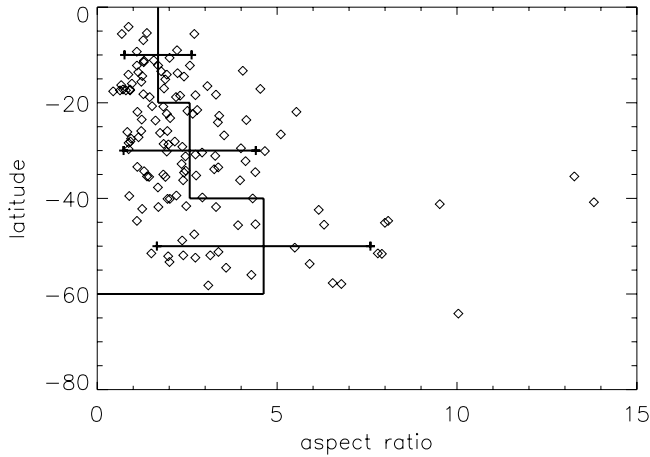


**Figure 5.** Aspect ratio (long axis divided by short axis) as a function of latitude. The data also have been binned into  $20^\circ$  latitude regions, with error bars indicating the standard deviation of aspect ratio in each region. One feature was identified poleward of  $60^\circ$ , which is shown in Figure 5, but obviously could not be sorted into any of the defined latitude bins.

observers [Crisp *et al.*, 1991a; Chanover *et al.*, 1998]. Low latitudes tend to be fairly bright, as well as middle to high latitudes (between about  $40^\circ$  to  $60^\circ$ ). There is typically less radiance emitted in middle to low latitudes (between about  $20^\circ$  and  $40^\circ$ ). The polar collar, which is not easily detected in ground-based observations, can be seen in these images as a region of significantly diminished radiance poleward of about  $60^\circ$ .

[31] Also shown in Figure 4, for comparison, is the estimated radiance at the location of the Pioneer Venus Large Probe. Although the Large Probe descended in the northern hemisphere, the location is plotted, in Figure 4, at about  $-5^\circ$  latitude. We assume a north-south atmospheric symmetry here because the planetary obliquity is only  $3^\circ$ , indicating minimal seasonal variations, and because previous observations are consistent with such a north-south symmetry, with only a few, probably transient, exceptions. Recent observations by Venus Express indicate that the dynamics of the south polar region are similar to those observed of the north polar region by Pioneer Venus, further supporting the likelihood of north-south hemispheric symmetry [Piccioni *et al.*, 2007]. This calculation of radiance experienced by the Pioneer Venus Large Probe assumes the cloud properties derived by Knollenberg and Hunten [1980], along with a factor of three reduction in the number of mode 3 particles [Pollack *et al.*, 1980]. This represents the radiance that results from a typical assumed set of Venus cloud properties and mass. The optical depth of the middle cloud (i.e., the optical depth below about 57 km) that was used to generate this radiance is approximately  $\tau \sim 23$ . This radiance is calculated using the model of McGouldrick and Toon [2007, 2008a, 2008b]. For a lack of an alternative, previous studies have taken this in situ observation (or reanalyses thereof) of the Venus cloud to be representative of the planetary cloud cover, as a whole [Toon *et al.*, 1982; Grinspoon *et al.*, 1993; James *et al.*, 1997; Imamura and

Hashimoto, 1998; McGouldrick and Toon, 2007]. Figure 4 shows that this clearly is not the case, since the predicted radiance of the cloud observed in situ by the Pioneer Venus Large Probe is closer to that of the maximum cloudiness (minimum radiance) encountered in the course of the 10 orbits analyzed here. Furthermore, the significant variability in radiance demonstrates the necessity of taking into account both the spatial and temporal cloud variability when determining the radiative balance of the middle atmosphere of Venus.

[32] As mentioned in section 1.2, Imamura and Hashimoto [1998] explained that the latitudinal brightness variations seen by Crisp *et al.* [1991a] likely were a consequence of the global-scale Hadley cell that exists in the atmosphere of Venus. The overall average of the latitudinal distribution of radiance in these data (solid line in Figure 4) is remarkably similar to the results of those simulations. The bright zone around  $50^\circ$  in the data corresponds with the minimum of opacity located around  $45^\circ$  in the simulations of Imamura and Hashimoto [1998]. The diminished radiance poleward of about  $60^\circ$  may be reaching a minimum around  $75^\circ$ . The location of this radiance minimum also corresponds well with the increase in opacity in the nominal simulations of Imamura and Hashimoto [1998], which peak around  $70^\circ$  to  $75^\circ$ . Imamura and Hashimoto [1998] also performed a simulation in which they reduced the effectiveness of the Hadley circulation by reducing by half the speed of the meridional circulation in their simulations. In contrast with the nominal simulation, this second simulation exhibited a peak of cloud opacity somewhat more equatorward, at about  $60^\circ$  latitude (compared with about  $75^\circ$  in their nominal simulation). Although the data considered here represent only 10 days worth of observation, these data indicate that, compared with their test case with reduced meridional speeds, the nominal case of Imamura and Hashimoto [1998] is a better representation of the Hadley circulation of Venus. The increase in the variability of the observed radiance at low latitudes is consistent with the observations by Crisp *et al.* [1991a] and also suggests the existence of significant convective activity in the clouds of Venus.

### 3.2. Latitudinal Distribution of Cloud Morphology

[33] In Figure 5, we plot the aspect ratio that we measured for approximately 130 features in the  $1.74 \mu\text{m}$  VIRTIS images from orbits 363 through 372, as a function of the latitude of the center of the feature. In addition to plotting each individually measured aspect ratio as symbols, we also bin the measured data into  $20^\circ$  latitude bins. The mean and standard deviation of these three bins are also plotted in Figure 5. We see in Figure 5 that the aspect ratio of the measured holes in the clouds increases with latitude. The typical hole becomes more elongated poleward of  $40^\circ$  (of the 16 features with aspect ratios greater than 5:1, all but three are poleward of  $40^\circ$ ). At low latitudes, in addition to holes having aspect ratios closer to 1.0, there also are several features with aspect ratios less than one (i.e., longer in the transverse direction than in the longitudinal direction), something that does not at all occur poleward of  $40^\circ$  in the images considered here. Thus, we observe a preponderance of highly elongated holes at high latitudes, and a

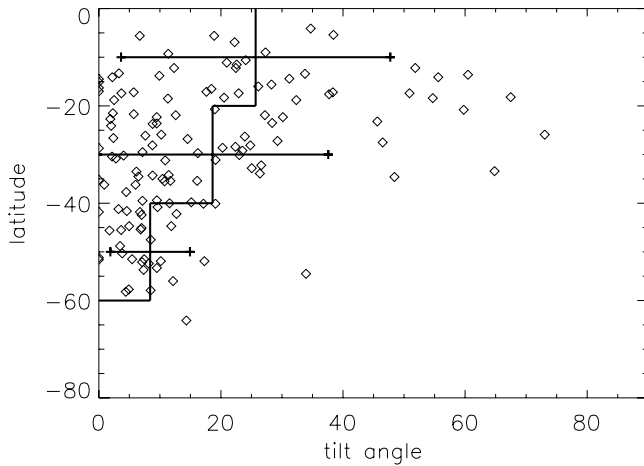


**Figure 6.** Tilt angle (relative to parallels of latitude) as a function of latitude. The data also have been binned into  $20^\circ$  latitude regions, with error bars indicating the standard deviation of tilt angle in each region. An angle of zero means zonally oriented features. The one feature poleward of  $60^\circ$  was not sorted into any bin.

tendency for more equal aspect ratios at lower latitudes. These results are consistent with the observations reported by *Belton et al.* [1991], as summarized in section 1.1.

[34] In Figure 6, we plot the angle that each feature makes relative to the parallels of latitude, as a function of latitude. A small “tilt angle” indicates that a feature is aligned nearly zonally, whereas a large tilt angle indicates a feature whose long axis is more vertically oriented. As in Figure 5, we plot each feature individually, as well as the mean and standard deviation of the tilt angle in  $20^\circ$  latitude bins. In Figure 6, we see that the average tilt angle is somewhat larger at low latitudes, becoming smaller at higher latitudes. This, in combination with the trends in Figure 5, indicates that the features not only become more elongated at higher latitudes, they also become more zonally oriented. There is significantly greater variation in the tilt angle at latitudes equatorward of  $40^\circ$ . The smaller variability poleward of  $40^\circ$  suggests that the polar vortex exerts its influence mainly on the poleward side of  $40^\circ$ . Furthermore, the variability equatorward of  $40^\circ$  suggests a complex interaction, likely involving convection, between the local atmospheric dynamics and the formation and evolution of the lower and middle clouds at lower latitudes.

[35] Figure 7 shows the peak radiance emerging from holes as a function of latitude. As in Figures 5 and 6, we plot both the individual features themselves, as well as the averages binned over  $20^\circ$  latitude bins. The mean of the feature peak radiance is about  $0.2 \text{ W m}^{-2} \mu\text{m}^{-1} \text{ sr}^{-1}$ , fairly consistent across all three latitude bins considered here. However, there is significantly more variability in the peak brightness of holes at low latitudes, as compared with the variability seen at higher latitudes. This too suggests that lower latitudes are demonstrating the effects of convection. Since the lower latitudes are viewed most obliquely in these data, the lower latitudes will be most affected by any errors that may occur in the correction for emission angle. However, even if our correction for the emission angle is flawed,

it will have affected the average brightness in this latitude bin, but not the variability.

### 3.3. Feature Lifetimes

[36] We might also be able to obtain information about the ages (and, ultimately, the lifetimes) of holes in the clouds from the morphology analyses. Recall, from equation (1), that the change in the atmospheric rotation period with latitude is a function of latitude only, if the zonal velocity is approximately constant. Cloud-tracking analysis by *Sánchez-Lavega et al.* [2008] suggests that the zonal wind is indeed a relatively constant  $60 \text{ m s}^{-1}$  at latitudes equatorward of about  $50^\circ$ . If we assume that a hole is circular when it is formed, and the zonal velocity is constant, then the poleward edge of the hole advances farther than the equatorward edge of the hole, at a rate given by equation (1) times the latitudinal extent of the hole ( $\Delta\phi$ ). If we assume that there is no meridional motion, then the ratio of this translation in degrees longitude to the latitudinal extent of the hole is precisely our previous definition of the tilt angle of the hole! For example, a circular hole centered at  $50^\circ$  latitude, having a meridional extent of  $2^\circ$ , exhibits a roughly  $3.15^\circ$  longitude  $\text{day}^{-1}$  difference between its top and bottom edges. After 1 day, this equates to a tilt angle of  $\theta = \tan^{-1}(2/3.15) = 32^\circ$ . After two days, the tilt angle would be  $18^\circ$ , and after three days,  $12^\circ$ . Granted, this is an extreme case. Holes that are closer to the equator experience less shearing because of this effect, since the angular velocity changes less quickly with latitude. A corresponding effect on the aspect ratio can also be calculated. Thus, these measurements of the aspect ratio and of the tilt angle, coupled with knowledge of the horizontal winds in the atmosphere, can provide a rough estimate of the ages of the holes in the clouds.

[37] Using the procedure outlined in section 2, we have identified 10 holes, in the series of images taken during orbit 383, whose evolution we have been able to analyze for this paper. This is such a small number of holes that it will be difficult to determine any global trends of hole evolution,

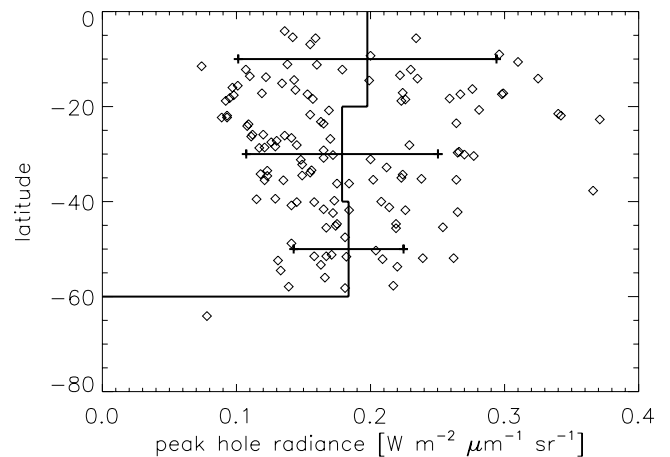


**Figure 7.** Peak radiance of the holes as a function of feature latitude. The data also have been binned into  $20^\circ$  latitude regions, with error bars indicating the standard deviation of feature peak radiance in each region. The one feature poleward of  $60^\circ$  was not sorted into any bin.

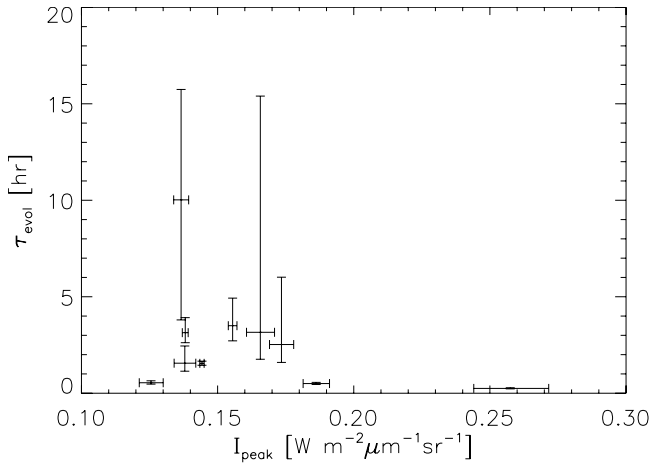


**Figure 8.** Derived evolutionary time scales versus peak radiance in the holes. Both axes are parameters of a log linear fit to the measured data. The error bars indicate the standard deviation error estimates of the fitted parameters.

whether as a function of position or size. Furthermore, the difficulty in establishing a method of hole definition that is consistent across successive images (i.e., that identifies the same hole, and is not fooled by changes in morphology or surroundings) may introduce small additional uncertainties. For the present investigation, we quantify these numerous error sources in the uncertainties of the fits to the data, as described in subsequent paragraphs. In future investigations we will improve the level of quantification of the error in these analyses of hole evolution, as well as improve our method of feature identification and tracking. Nevertheless, as the first quantitative measurement of cloud evolution, this analysis provides the first benchmark of the lifetimes of the holes in the clouds of Venus.

[38] We fit the sequence of the measured peak radiance for each hole according to an exponential variation:

$$\ln I_{peak}(t) = \ln I_{peak}(0) - \frac{1}{\tau} t \quad (2)$$

where the initial peak radiance [ $\ln I_{peak}(0)$ ] and the evolutionary time constant ( $\tau$ ) are free parameters to be fit to the data for each hole. We find that, for the holes we have analyzed during orbit 383, the average time scale for evolution of a typical hole is  $0.95^{+4.88}_{-0.51}$  days. Thus, since the typical e-folding time scale of a hole is approximately 1 day, the peak radiance of a typical hole will decrease to approximately 1% of its initial value in a time of about 4.5 days. Note, however, that there is a large upper error bar to this time scale, indicating that a significant fraction of holes can be expected to exhibit time constants for evolution as large as 5–6 days. Such slowly evolving holes will remain evident for many weeks.

[39] Figure 8 shows the relationship between the initial peak radiance and the evolutionary time scale. Each point in Figure 8 represents the best linear fit to equation (2) for each measured hole. The vertical error bars indicate the one standard deviation variation in the slope ( $1/\tau$ ), and the horizontal error bars indicate the one standard deviation variation in the initial peak radiance [ $I_{peak}(0)$ ]. Note that the initial peak radiance in this case refers to the peak radiance

fit to the curve at the time of the first image acquisition. It does not represent an actual measurement of radiance, nor does the variance shown indicate a known measurement error. Figure 8 may exhibit a peak in the evolutionary time constant (i.e., both thicker and thinner holes than this tend to evolve more quickly) at about  $I_{peak} \sim 0.15 \text{ W m}^{-2} \mu\text{m}^{-1} \text{ sr}^{-1}$ . However, the small number of holes that have been analyzed, and the large error bars on some of the features, cause us to have only a little confidence in the existence of such a peak, at this time.

[40] For Figure 9 we replace  $I_{peak}$  in equation (2) with the contrast between the peak radiance and the background radiance. We define the contrast as the ratio between the peak radiance of the hole (which we have measured directly from the images), and the local background radiance. We determine the local background radiance to be the mean minus one standard deviation of the radiance in the image at the latitude of the center of the hole. Recall from Figure 4 that the mean minus one standard deviation as a function of latitude tracks remarkably close to the minimum radiance as a function of latitude. Thus, the mean minus one standard deviation stands as a reasonable proxy for the minimum radiance (or thickest cloud cover). In Figure 9, we see a possible trend indicating that holes with greater contrast evolve more quickly than holes with smaller contrast. This is consistent with simulations of hole evolution [McGouldrick and Toon, 2008b]. It also suggests that a uniform cloud cover is the equilibrium situation in the Venus atmosphere, since large contrasts between cloudy and clear regions are quickly reduced, and small contrasts evolve rather slowly.

[41] In Figure 10, we plot the evolution time constant obtained from the analysis of the peak radiance as a function of the latitude of the analyzed holes. In Figure 10, the horizontal error bars indicate the range of latitudes at which a given measured hole was located during the course of the image sequence. That is, a large horizontal error bar may be indicative of a significant meridional motion. If meridional

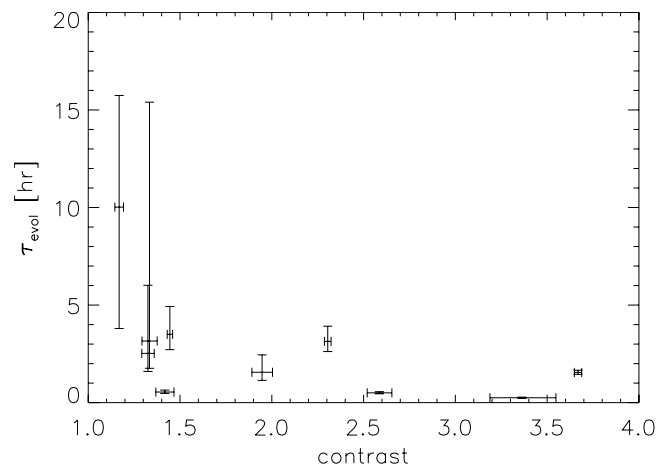


**Figure 9.** Derived evolutionary time scales versus contrast between the peak hole radiance and the background radiance. Background radiance is defined in the text. Both axes are parameters of a log linear fit to the measured data. The error bars indicate the standard deviation error estimates of the fitted parameters.

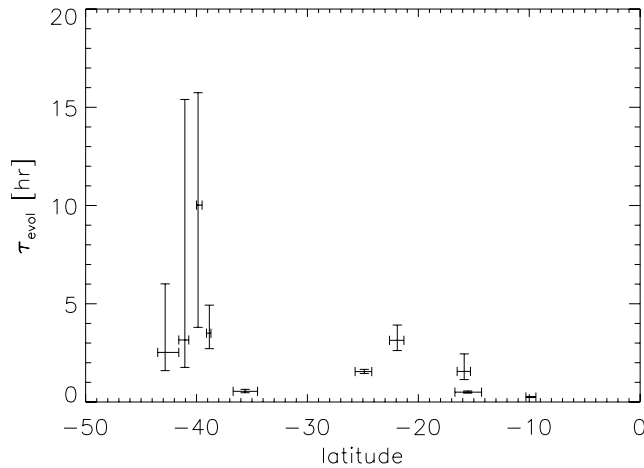


**Figure 10.** Derived evolutionary time scales versus the latitudes of the measured holes. The horizontal error bars indicate the range of latitudes measured for each hole during the sequence of images. The vertical error bars indicate the standard deviation error estimates of the fitted time scale.

motion can be ruled out, then a significant variation in measured feature latitude suggests that we may not be measuring the same feature in each image. With sufficient statistics and independent means of determining wind velocities, such an analysis can provide a further check on the validity of the analysis of feature evolution. Even with the small number of features measured in this instance, there appears to be a trend in which holes at lower latitudes evolve more quickly than those at higher latitudes. This behavior is consistent with the earlier assessment of increased cloud variability at equatorial latitudes.

[42] In each of these analyses, our conclusions are necessarily tentative, as they derive from measurements of only 10 holes over the span of only 5 h. We hope to improve on these statistics by measuring many more features in many more images in the future. Nevertheless, these analyses represent a first quantitative assessment of the evolution of holes in the middle and lower clouds of Venus.

#### 4. Conclusions

[43] We have analyzed a series of ten  $1.74 \mu\text{m}$  VIRTIS-M IR images, taken on successive orbits, covering a span of 10 days, to identify tendencies to the morphology and the brightness of the holes in the clouds of Venus. We have also analyzed a separate series of eleven  $1.74 \mu\text{m}$  VIRTIS-M IR images, taken over the course of a single orbit, spanning a time of 5 h, to investigate the evolution of the holes in the clouds of Venus.

[44] We find that the latitudinal distribution of radiance in which midlatitudes are relatively brighter, and low latitudes exhibit somewhat greater overall variability, is consistent with that observed by *Crisp et al.* [1991a], indicating that this tendency is a fairly stable phenomenon. The latitudinal distribution of average radiance that we observe in the images considered here is largely consistent with the simulations of *Imamura and Hashimoto* [1998], indicating that the global Hadley circulation plays a significant role in the distribution of the cloud mass of Venus. We observe an

increase in the variability of radiance at lower latitudes, suggestive of the importance of convection to the nature of the middle and lower clouds of Venus. While the distribution of potential cloud constituents and their precursors (i.e.,  $\text{H}_2\text{SO}_4$ ,  $\text{SO}_2$ ,  $\text{H}_2\text{O}$ , and amorphous sulfur) are not constrained by the data and analyses presented here, variations in these constituents, driven either by chemistry or by the atmospheric dynamics already noted, might also play a role in the cloud variability.

[45] We find that the morphology of the holes in the clouds of Venus trends from features having a wide variety of orientations (relative to the zonal axis) and aspect ratios of approximately 1.0 at lower latitudes, to highly elongated and zonally oriented features at high latitudes. The greater variability in the morphology of features at lower latitudes is possibly indicative of a greater amount of convective activity there. We fail to find a correlation between the peak radiance of a hole and its latitude. A hint of a longitudinal hemispheric asymmetry, similar to that observed by *Crisp et al.* [1991a] and *Chanover et al.* [1998] was seen; but the amount of data considered here is insufficient to be certain of its existence here.

[46] We find that, if the data analyzed here are typical, holes in the middle and lower clouds of Venus evolve with a time constant of approximately 1 day. We find that holes exhibiting greater contrast between their peak radiance and the background radiance, and holes at lower latitudes evolve more quickly. This is consistent with the increased variability seen at lower latitudes that results from enhanced convection. It is also consistent with the notion that the middle and lower clouds are supported by a radiative dynamical feedback, whereby regions exhibiting large contrasts in clouds cover will also experience large contrasts in radiative heating because of the absorption of upwelling infrared radiation. However, the data considered here represent only 5 h of observation of a fairly small area (about 2% of the atmosphere). This is hardly sufficient data to allow us to draw any broad conclusions. We intend to carry out future efforts to improve both the methods of the analysis as well as the volume of analyzed data.

[47] The features in the images analyzed here strongly indicate the activity of convection in the lower and middle cloud decks of Venus. The spatial variability and short time scale for their evolution are somewhat inconsistent with typical terrestrial stratus, to which the clouds of Venus are often compared. However, previous radiative modeling by *Pollack et al.* [1980] and microphysical modeling of the middle and lower clouds by *McGouldrick and Toon* [2007] suggests the existence of a radiative dynamical feedback, which can support convection in the lower and middle cloud decks of Venus. The clouds of Venus may be more analogous to terrestrial stratocumulus “cloud streets,” whereby convection exists in the midst of strong horizontal flow [*Houze*, 1993]. Depending upon the relative strengths of the horizontal flow and the convection, either rolls or cellular patterns may be formed. Similarly, the nature of terrestrial thunderstorm development (whether single-cell, multicell, or supercell) is known to be somewhat dependent upon the local wind shear and static stability [*Houze*, 1993]. Perhaps processes analogous to cloud street formation or the development of multicell thunderstorms are occurring in the atmosphere of Venus in the vicinity of the lower and middle clouds.

[48] Here we have presented analyses of only a small subset of the VIRTIS data. We have analyzed data from only 11 orbits, from among more than 500: barely 2% of the total available VIRTIS data set. However, given that at this writing, Venus Express has been orbiting Venus for more than three full Venus years, there likely is sufficient data in the archive to seek out potential tendencies of hole formation and/or appearance as a function of geographic or solar longitude. We intend to carry out further analyses of the VIRTIS data to determine whether such tendencies exist. Furthermore, comparisons with observations at other wavelengths, and concurrent Venus Monitoring Camera observations, can be utilized to gain greater understanding of the properties and evolution of the Venus clouds. In the longer term, the anticipated arrival of the Japanese Space Agency's Venus Climate Orbiter (VCO) in 2010 promises to enhance the study of the Venus clouds [Nakamura *et al.*, 2007]. The understanding of the nature of the middle and lower clouds of Venus could gain much from the potential coordinated observation of Venus by the two spacecraft. Subsequent observations of the same region of the atmosphere could extend the analysis of cloud evolution beyond the limits that either VCO or Venus Express could accomplish by itself, by extending the baseline of time over which a particular feature is viewable. Concurrent observations of features by multiple spacecraft could further elucidate the cloud properties. For example, it may be possible to determine the difference between the properties of a profile of a hole versus that of a cloud by performing occultation measurements with one spacecraft, while the other identifies the types of features that are passing over the limb of the planet. Alternately, long-lived balloon observatories can be placed in the atmosphere and possibly maneuvered to sample the atmosphere in regions that are identified by the concurrently orbiting spacecraft.

[49] **Acknowledgments.** We thank two anonymous reviewers for their careful reading of the manuscript and their suggestions for making this a stronger paper. We also acknowledge conversations with Colin Wilson, Con Tsang, and Robert Carlson that have helped to improve the analysis of the data with respect to the correction for the emission angle. We also thank The European Space Agency for the opportunity to work with Venus Express. We thank Pierre Drossart, Giuseppe Piccioni, and the VIRTIS team for their assistance in enabling us to reduce and analyze the VIRTIS data. A portion of the work described in this paper was carried out at the Jet Propulsion Laboratory, Pasadena, California, under contract with NASA. K.M. and D.H.G. were supported by NASA in support of ESA's Venus Express mission under grant NNX07AI61G.

## References

- Allen, D. A., and J. W. Crawford (1984), Cloud structure on the dark side of Venus, *Nature*, *307*, 222–224.
- Baker, R. D., G. Schubert, and P. W. Jones (2000), Convectively generated internal gravity waves in the lower atmosphere of Venus, part II: Mean wind shear and wave-mean flow interaction, *J. Atmos. Sci.*, *57*, 200–215.
- Belton, M. J. S., et al. (1991), Images from Galileo of the Venus cloud deck, *Science*, *253*, 1531–1536.
- Blamont, J. E., et al. (1986), Implications of the VEGA balloon results for Venus atmospheric dynamics, *Science*, *231*, 1422–1425.
- Bullock, M. A., and D. H. Grinspoon (2001), The recent evolution of climate on Venus, *Icarus*, *150*, 19–37, doi:10.1006/icar.2000.6570.
- Carlson, R. W., et al. (1991), Galileo infrared imaging spectroscopy measurements at Venus, *Science*, *253*, 1541–1548.
- Carlson, R. W., L. W. Kamp, K. H. Baines, J. B. Pollack, D. H. Grinspoon, Th. Encrenaz, P. Drossart, and F. W. Taylor (1993), Variations in Venus cloud particle properties: A new view of Venus's cloud morphology as observed by Galileo Near-Infrared Mapping Spectrometer, *Planet. Space Sci.*, *41*, 477–485, doi:10.1016/00320633(93)900306.

- Chanover, N. J., D. A. Glenar, and J. J. Hillman (1998), Multispectral near-IR imaging of Venus nightside cloud features, *J. Geophys. Res.*, *103*, 31,335–31,348.
- Counselman, C. C., S. A. Gourevitch, R. W. King, G. B. Loroit, and E. S. Ginsberg (1980), Zonal and meridional circulation of the lower atmosphere of Venus determined by radio interferometry, *J. Geophys. Res.*, *85*, 8026–8030.
- Crisp, D. (1989), Radiative forcing of the Venus mesosphere, *Icarus*, *77*, 391–413, doi:10.1016/00191035(89)900961.
- Crisp, D., et al. (1989), The nature of the near-infrared features on the Venus night side, *Science*, *246*, 506–509.
- Crisp, D., D. A. Allen, D. H. Grinspoon, and J. B. Pollack (1991a), The dark side of Venus: Near-infrared images and spectra taken from the Anglo-Australian Observatory, *Science*, *253*, 1263–1266.
- Crisp, D., et al. (1991b), Ground-based near-infrared imaging observations of Venus during the Galileo encounter, *Science*, *253*, 1538–1541.
- Drossart, P., et al. (2007), Scientific goals for the observation of Venus by VIIS on ESA/Venus Express mission, *Planet. Space Sci.*, *55*, 1653–1672, doi:10.1016/j.pss.2007.01.003.
- Grinspoon, D. H., J. B. Pollack, B. R. Sitton, R. W. Carlson, L. W. Kamp, K. H. Baines, Th. Encrenaz, and F. W. Taylor (1993), Probing Venus's cloud structure with Galileo NIMS, *Planet. Space Sci.*, *50*, 515–542, doi:10.1016/00320633(93)90034Y.
- Hashimoto, G. L., and Y. Abe (2000), Stabilization of Venus' climate by a chemical-albedo feedback, *Earth Planets Space*, *52*, 197–202.
- Hinson, D. P., and J. M. Jenkins (1995), Magellan radio occultation measurements of atmospheric waves on Venus, *Icarus*, *114*, 310–327, doi:10.1006/icar.1995.1064.
- Houze, R. A. (1993), *Cloud Dynamics*, Academic, San Diego, Calif.
- Imamura, T., and G. L. Hashimoto (1998), Venus cloud formation in the meridional circulation, *J. Geophys. Res.*, *103*, 31,349–31,366.
- James, E. P., O. B. Toon, and G. Schubert (1997), A numerical microphysical model of the condensational Venus cloud, *Icarus*, *129*, 147–171, doi:10.1006/icar.1997.5763.
- Knollenberg, R. G., and D. H. Hunten (1980), The microphysics of the clouds of Venus: Results of the Pioneer Venus Particle Size Spectrometer Experiment, *J. Geophys. Res.*, *85*, 8038–8058.
- Linkin, V. M., et al. (1986), Vega balloon dynamics and vertical winds in the Venus middle cloud region, *Science*, *231*, 1417–1419.
- Markiewicz, W., et al. (2007a), Venus Monitoring Camera for Venus Express, *Planet. Space Sci.*, *55*, 1701–1711, doi:10.1016/j.pss.2007.01.004.
- Markiewicz, W. J., et al. (2007b), Morphology and dynamics of the upper cloud layer of Venus, *Nature*, *450*, 633–636, doi:10.1038/nature06320.
- McGouldrick, K., and O. B. Toon (2007), Investigation of possible causes of the holes in the condensational Venus cloud using a microphysical cloud model with a radiative-dynamical feedback, *Icarus*, *191*, 1–24, doi:10.1016/j.icarus.2007.04.007.
- McGouldrick, K., and O. B. Toon (2008a), Observable effects of convection and gravity waves on the Venus condensational cloud, *Planet. Space Sci.*, *46*, 1112–1131, doi:10.1016/j.pss.2008.02.010.
- McGouldrick, K., and O. B. Toon (2008b), Modeling the effects of shear on the evolution of the holes in the condensational clouds of Venus, *Icarus*, *196*, 35–48, doi:10.1016/j.icarus.2008.02.020.
- Nakamura, M., et al. (2007), Planet-C: Venus Climate Orbiter mission of Japan, *Planet. Space Sci.*, *55*, 1831–1842, doi:10.1016/j.pss.2007.01.009.
- Piccioni, G., et al. (2007), South-polar features on Venus similar to those near the north pole, *Nature*, *450*, 637–640, doi:10.1038/nature06209.
- Pollack, J. B., O. B. Toon, and R. Boese (1980), Greenhouse models of Venus' high surface temperature, as constrained by Pioneer Venus measurements, *J. Geophys. Res.*, *85*, 8223–8231.
- Sánchez-Lavega, A., et al. (2008), Variable winds on Venus mapped in three dimensions, *Geophys. Res. Lett.*, *35*, L13204, doi:10.1029/2008GL033817.
- Schubert, G., et al. (1980), Structure and circulation of the Venus atmosphere, *J. Geophys. Res.*, *85*, 8007–8025.
- Taylor, F. W., et al. (1979), Temperature, cloud structure, and dynamics of Venus middle atmosphere by infrared remote-sensing from pioneer orbiter, *Science*, *205*, 65–67.
- Toon, O. B., R. P. Turco, and J. B. Pollack (1982), The ultraviolet absorber on Venus: Amorphous sulfur, *Icarus*, *51*, 358–373, doi:10.1016/00191035(82)900896.

K. H. Baines and T. W. Momary, Jet Propulsion Laboratory, California Institute of Technology, M/S 183-601, 4800 Oak Grove Drive, Pasadena, CA 91109, USA.

D. H. Grinspoon and K. McGouldrick, Department of Space Sciences, Denver Museum of Nature and Science, 2001 Colorado Boulevard, Denver, CO 80205, USA. (kmcgouldrick@dmns.org)